Carbohydrate Polymers 113 (2014) 9–15

Contents lists available at ScienceDirect

Carbohydrate Polymers

journal homepage: www.elsevier.com/locate/carbpol

Investigation of inclusion complex of honokiol with sulfobutyl ether-β-cyclodextrin

Caibing Xu[a], Yalan Tang[a], Wenjing Hu[b], Rui Tian[c], Yuntao Jia[d], Ping Deng[a], Liangke Zhang[a,*]

[a] Chongqing Key Laboratory of Biochemistry and Molecular Pharmacology, School of Pharmacy, Chongqing Medical University, Chongqing 400016, PR China
[b] Chongqingshi Shapingba District People's Hospital, Chongqing 400030, PR China
[c] The Experimental Teaching Centre, Chongqing Medical University, Chongqing 400016, PR China
[d] Department of Pharmacy, Children's Hospital of Chongqing Medical University, Chongqing 400010, PR China

ARTICLE INFO

Article history:
Received 20 February 2014
Received in revised form 1 June 2014
Accepted 14 June 2014
Available online 1 July 2014

Keywords:
Sulfobutyl ether-β-cyclodextrin
Honokiol
Inclusion complex
In vitro release
Pharmacokinetic study

ABSTRACT

This study aimed to prepare and characterize an inclusion complex of honokiol (HNK) with sulfobutyl ether-β-cyclodextrin (SB-β-CD). The inclusion complex (HNK/CD COMP) was prepared utilizing a freeze–drying method. Phase-solubility curves were employed to obtain stability constants and thermodynamic parameters. The phase-solubility diagram showed a typical A_L-type, indicating that the 1:1 (HNK:SB-β-CD) inclusion complex was formed. The solid inclusion complex was then characterized by differential scanning calorimetry and Fourier transform infrared spectroscopy. Results showed that HNK/CD COMP exhibited a higher drug release rate than free HNK in vitro. A comparative study of the pharmacokinetics between HNK/CD COMP and free HNK was also performed in rats. In vivo results indicated that AUC_{0-t} and C_{max} of HNK/CD COMP increased by approximately 158% and 123% compared with those of the free HNK, respectively. These results suggest that SB-β-CD will be potentially useful in the delivery of poorly soluble drugs, such as HNK.

1. Introduction

Cyclodextrins (CDs) are a family of macrocyclic oligosaccharides mostly consisting of six, seven, or eight glucose units joined by α-1,4 glycosidic bonds (Brewster & Loftsson, 2007; Stella & He, 2008). The hydrophobic cavity of CDs provides these CDs the ability to form inclusion complexes with various compounds, including proteins, oligonucleotides, ions, and small molecules (Stella & He, 2008; Zhang & Ma, 2013). As a promising material with low toxicity and low immunogenicity, CDs have been extensively investigated in the field of biomedicine, particularly in pharmaceutical sciences and technologies. Related applications include the improvement of drug solubility and stability, increase in drug absorption and bioavailability, removal of odors and tastes, and decrease in local and systemic toxicity (Carrier, Miller, & Ahmed, 2007; Garcia-Fernandez et al., 2013; Zhang & Ma, 2013). CDs can be administered by oral, ocular, nasal, and rectal delivery (Al-Rawashdeh, Al-Sadeh, & Al-Bitar, 2010; Pahuja, Kashyap, & Pawar, 2014; Singh, Kumar, & Pathak, 2013; Tiwari, Tiwari, & Rai, 2010). To improve these properties of natural CDs in terms of solubility, stability, inclusion capability, and toxicity, researchers synthesized various chemically modified CDs, such as amphiphilic, hydrophobic, and highly soluble derivatives.

When new excipients are considered as drug carries, safety should be primary concern. Unmodified cyclodextrins, such as α- and β-cyclodextrin, were extensively investigated in pharmaceuticals. However, they were limited by hemolytic activity and nephrotoxicity because of their interaction with cholesterol and other lipid membrane components of cellular structures (Luke, Tomaszewski, Damle, & Schlamm, 2010).

Sulfobutyl ether-β-cyclodextrin (SB-β-CD, Fig. 1A) is an excellent modified compound of β-cyclodextrin with improved water solubility and low toxicity. SB-β-CD does not undergo significant tubular reabsorption due to its ionized state after glomerular filtration and is concentrated in the urine for excretion, which attenuate the potential to harm the kidney (Albers & Muller, 1995; Irie & Uekama, 1997; Uekama, 2004). SB-β-CD can form inclusion complexes with drug molecules. Thus, SB-β-CD has been utilized to improve the solubility and stability of drugs (Danel et al., 2013; Stella & He, 2008; Venuti et al., 2013).

* Corresponding author at: School of Pharmacy, Chongqing Medical University, District of Yuzhong, Chongqing 400016, PR China. Tel.: +86 23 6848 5161; fax: +86 23 6848 5161.
E-mail address: zlkdyx@gmail.com (L. Zhang).

http://dx.doi.org/10.1016/j.carbpol.2014.06.059
0144-8617/

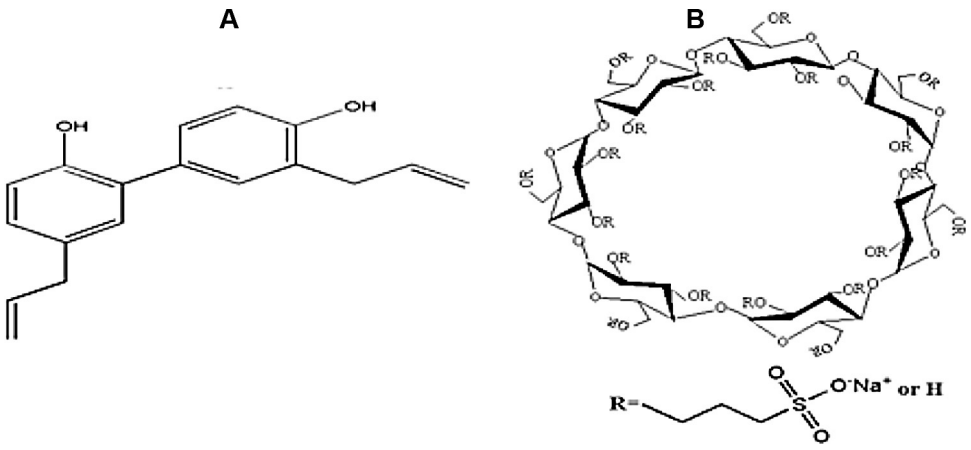

Fig. 1. The chemical structure of HNK (A) and SB-β-CD (B).

Honokiol (HNK, Fig. 1B) is a bioactive lignanoid extracted from the reed of *Magnolia officinalis*, which has been utilized in traditional Chinese medicine for a long time. Furthermore, HNK is extensively used in Japan (Cheng, 2012; Lee et al., 2011). This compound exhibits several pharmacological properties, such as anti-cancer effects, anti-inflammatory effects, anti-oxidant actions, and anti-anxiety effects. However, the poor aqueous solubility of HNK has impeded clinical applications (Choi et al., 2002; Kang et al., 2008; Weeks, 2009; Yamaguchi, Satoh-Yamaguchi, & Ono, 2009).

In this study, the inclusion complex of HNK and SB-β-CD (HNK/CD COMP) was prepared to improve the solubility and bioavailability of HNK using a freeze–drying method (Jadhav, Petkar, Pore, Kulkarni, & Burade, 2013; Rajendiran & Siva, 2014; Zhang et al., 2013). Solid-state HNK/CD COMP was characterized by differential scanning calorimetry (DSC) and Fourier transform infrared spectroscopy (FT-IR). In a solution, solubility phase analysis was performed to estimate the enhanced solubility of HNK by SB-β-CD and the stoichiometry of the inclusion complex. In vitro release study and model fitting were systematically investigated and evaluated. Furthermore, the pharmacokinetic properties of HNK suspension and HNK/CD COMP in male Sprague-Dawley rats were analyzed.

2. Materials and methods

2.1. Materials

Honokiol (purity ≥ 98%) was purchased from Xi'an Grass Plant Science and Technology Co., Ltd. (Xi'an, China). SB-β-CD (DS = 7.0) was purchased from Shandong Binzhou Zhiyuan Bio-Technology Co., Ltd. (Shandong, China). All the other reagents were of analytical grade.

2.2. Phase-solubility analysis

Phase-solubility analysis was performed in a SHZ-88 thermostatic shaking water bath (Jiangsu Taicang Medical Instrument Factory, China). The excess amount of HNK was added to volumetric flasks containing 10 mL of SB-β-CD solutions at various concentrations (0, 5, 10, 15, 20, 25, and 30 mM). The contents were then sonicated for 5 min. The flasks were sealed to prevent evaporation and shaken continuously at 100 rpm in a thermostatic bath at different temperatures (25, 37, and 50 °C) for 48 h. After equilibrium was reached, suspensions were filtered using a 0.45 μm syringe filter. The amount of drug was then analyzed at a wavelength of 292 nm by using a spectrophotometer (Shimazdu UV-3150, Japan). Experiments were performed in triplicate.

2.3. Preparation of inclusion complex

The inclusion complex was prepared using a freeze–dry method (Pralhad & Rajendrakumar, 2004; Ruz et al., 2012; Wang, Luo, & Xiao, 2014). On the basis of the results of phase-solubility analysis, we dispersed 100 mg of HNK in 100 mL of water containing 1.68 g of SB-β-CD at 45 °C. After magnetically stirring for 2.5 h, we filtered the resultant solution with a 0.45 μm syringe filter and the filtrate was freeze-dried (ALPHA 1-2 LD plus, CHRIST, Germany) for 48 h.

2.4. DSC

DSC measurements were performed to confirm that the complex was formed. The powdered samples of HNK, SB-β-CD, HNK/CD COMP, and physical mixture (HNK/CD PM) were placed in an aluminum pan, heated to 70 °C for 5 min, and cooled to 20 °C for 5 min at the cooling rate of 10 °C min^{-1}. And then the profiles were obtained by using a Netzsch STA449C thermal analyzer (Netzsch Corporation, Germany) from 20 °C to 300 °C (at a constant rate of 10 °C min^{-1}) under nitrogen gas flow (25 mL min^{-1}).

2.5. Fourier transform infrared spectroscopic (FT-IR) study

The FT-IR spectra of the powdered samples of HNK, SB-β-CD, HNK/CD COMP, and HNK/CD PM were obtained using a spectrometer (Bruker-tensor 27, Germany) with the potassium bromide pellet method. The typical bands were recorded for different samples. Each spectrum was recorded in the range of 4000 to 400 cm^{-1}. The spectra were obtained under dry conditions at a resolution of 4 cm^{-1} to prevent contamination.

2.6. Dissolution studies

Dissolution studies were implemented using the dialysis membrane method. Three formulations, namely, HNK, HNK/CD PM, and HNK/CD COMP were transferred into a dialysis bag (molecular weight cutoff, 8–14 kDa). The dialysis bag was then immersed in a container filled with 25 mL of 0.1 mM phosphate buffer solution (pH 7.4) containing sodium dodecyl sulfate (SDS, 0.5%) at 37 °C with constant shaking (100 rpm). The receptor compartments were closed to prevent the dissolution medium from evaporating. An aliquot (4.0 mL) of the incubation medium was withdrawn and replaced with the same volume of pre-warmed fresh medium at specific time intervals. The concentration of HNK was then determined using a UV spectrophotometer (Shimazdu UV-3150, Japan) after HNK was filtered using a 0.45 μm membrane. The cumulative

release percentage (Q) was calculated according to the following equation:

$$Q = \frac{\left(C_n \times 25 + \sum_{i=1}^{n-1} C_i \times 4\right)}{A} \times 100\% \quad (1)$$

where n and i are the sample numbers, C_n and C_i are the drug concentration at the point of n and i, respectively, and A is the total drug content in each sample.

Similarity factor (f_2) was first proposed by Moore and Flanner (Costa & Sousa Lobo, 2001; Shah, Tsong, Sathe, & Liu, 1998) to compare release profiles. It was derived from Mean-Squared difference. Similarity factor (f_2) was also recommended for release profile comparison in the FDA's Guidances for Industry (FDA, 1997; Shah et al., 1997). In this study, f_2 was used to evaluate the similarity between every two release profiles. The factor f_2 is defined by the following equation:

$$f_2 = 50 \times \lg\left\{\left[1 + \left(\frac{1}{n}\right)\sum_{t=1}^{n}(R_t - T_t)^2\right]^{-0.5} \times 100\right\} \quad (2)$$

where n is the number of sampling points, and R_t and T_t are HNK cumulative release percentages at time t of the two release curves, respectively. The result indicated that the similarity between the two release profiles was statistically significant at $f_2 > 50$. A high similarity between two profiles is characterized by a high f_2.

2.7. Pharmacokinetic analysis in rats

2.7.1. Animal handling and care

Male Sprague-Dawley rats weighing approximately 200 ± 20 g were obtained from the Laboratory Animal Center of Chongqing Medical University and used for pharmacokinetic analysis. The animal experiment was approved by the Animal Ethics Committee of Chongqing Medical University (Chongqing, China), and their guidelines were followed throughout this study. Before the experiment was conducted, the rats were fasted overnight but provided free access to water.

2.7.2. Pharmacokinetic behavior of rats

Eighteen rats were randomly divided into three groups, namely, A, B, and C (n = 6 rats). Group A received a single oral dose of HNK/CD COMP (80 mg kg^{-1} of HNK) and group B was orally administered a single dose of HNK suspension (80 mg kg^{-1} of HNK suspended in 0.5% sodium carboxymethyl cellulose solution). The blood samples (0.5 mL) were collected at 0.083, 0.25, 0.5, 1, 2, 4, 6, 10, 12, 24, and 48 h post-treatment.

Group C was injected with the HNK/CD COMP solution at a dose of 20 mg kg^{-1} of HNK in the tail vein. The blood samples (0.5 mL) were collected from the retro-orbital plexus of each rat and transferred into heparinized tubes at 0.033, 0.083, 0.25, 0.5, 0.75, 1, 1.5, 2, 4, and 6 h post-administration. These samples were immediately centrifuged, and the plasma samples were stored at −20 °C for further studies.

2.7.3. Preparation of plasma samples

An aliquot of plasma (200 μL) was pre-treated with 20 μL of evodiamine methanol solution (20 μg mL^{-1}) as an internal standard and then vortexed for 5 min. The resulting sample was mixed with 1.5 mL of ethyl acetate, vortexed for another 5 min, and centrifuged at 4000 rpm for 10 min. Afterward, the supernatant was evaporated to dryness in a vacuum, redissolved in 100 μL of methanol, and centrifuged at 12,000 rpm for 10 min. This sample solution (20 μL) was directly injected into a HPLC system (Agilent 1100, American) for analysis.

2.7.4. Measurement of HNK from plasma using RP-HPLC

The plasma concentrations of HNK were determined by an Agilent 1100 HPLC system (Agilent, American). A Lichrospher RP C_{18} column (4.6 mm × 150 mm, 5 μm, Hanbon Sci. & Tech., China) was used and the mobile phase was a mixture of methanol and water (80:20, v/v). The flow rate was 1.0 mL min^{-1}. All of the detections were performed at a wavelength of 292 nm at a constant temperature of 30 °C.

2.7.5. Pharmacokinetic analysis

The valuable pharmacokinetic parameters, namely, AUC_{0-t} (area under the plasma concentration versus time curve), C_{max} (peak drug concentration), T_{max} (time to reach the peak concentration), V_d (apparent volume of distribution), $t_{1/2}$ (half-life), and CL (clearance) were collected by DAS2.1.1 (issued by the China Food and Drug Administration for pharmacokinetic study). All data were presented as the mean ± standard deviation (n = 6, $\bar{x} \pm s$).

3. Results and discussion

3.1. Phase solubility study

Phase-solubility study is a traditional and useful approach not only to determine the value of the stability constant, but also to give insight into the stoichiometry of the equilibrium. The practical and phenomenological implications of phase solubility study were developed by Higuchi and Connons (Higuchi & Connors, 1965). Based on the profiles of the phase solubility study, several types of solubility behaviors can be classified. The phase solubility diagrams include two major types: A type (a soluble compound was formed) and B type (a compound of limit solubility was formed) (Brewster & Loftsson, 2007; Thompson, 1997).

In this study, phase-solubility study was performed to determine the interactions between HNK and SB-β-CD. The study infused the solubilizing ability of SB-β-CD to HNK and the stability constant of HNK/CD COMP according to the phase-solubility diagram. Fig. 2 shows the phase solubility diagrams of HNK and SB-β-CD in three different temperatures. All of the apparent solubility curves of HNK with correlation coefficient r > 0.9963 were regarded as straight lines. Moreover, all of them can be considered as A_L-type diagrams, indicating that the observed increase in the solubility of HNK was due to the formation of a 1:1 molar ratio inclusion complex.

The inclusion stability constant $K_{1:1}$ was calculated using the following equation (Brewster & Loftsson, 2007; Thompson, 1997):

$$K_{1:1} = \frac{\text{Slope}}{S_0(1 - \text{Slope})} \quad (3)$$

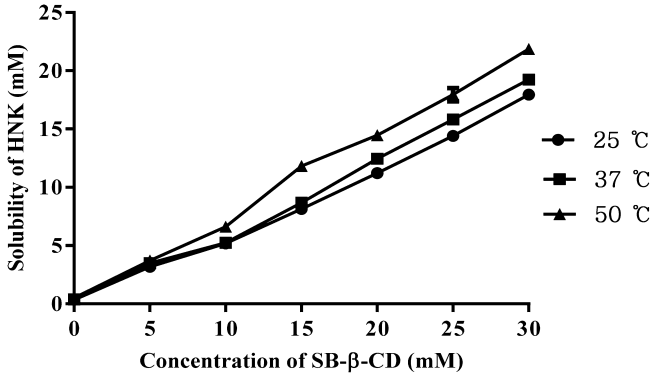

Fig. 2. Phase solubility diagram of HNK and SB-β-CD at 25, 37, and 50 °C (n = 3, error bars are smaller than symbols).

Table 1
The main thermodynamic parameters of HNK/SBECD.

Temperature (°C)	Regression equation	$K_{1:1}$ (L mol^{-1})	ΔG (kJ mol^{-1})	ΔH (kJ mol^{-1})	ΔS (J (mol K)$^{-1}$)
25	$y = 0.580x - 0.077$, ($r = 0.9972$)	3945	−20.525		
37	$y = 0.631x - 0.144$, ($r = 0.9963$)	4407	−21.636	7.765	94.86
50	$y = 0.717x + 0.239$, ($r = 0.9979$)	5027	−22.636		

where S_0 is the equilibrium solubility of HNK in water; slope is obtained from the phase-solubility diagram. $K_{1:1}$ at 25, 37, and 50 °C was calculated from Eq. (3). Thermodynamic parameters were calculated from Gibbs and Van't Hoff equations:

$$\Delta G = -RT \ln K_{1:1} \quad (4)$$

$$\ln K_{1:1} = \frac{-\Delta H}{RT} + \frac{\Delta S}{R} \quad (5)$$

Valuable parameters, including stability constant ($K_{1:1}$), Gibbs free energy change (ΔG), enthalpy change (ΔH), and entropy change (ΔS), are listed in Table 1. $K_{1:1}$ increased with rising temperature. ΔG of HNK was negative and decreased as temperature increased. ΔH was positive in this study. The thermodynamic parameters and $K_{1:1}$ indicated that high temperatures were favorable for the inclusion process (Hu, Zhang, Song, Gu, & Hu, 2012; Rajendiran & Siva, 2014).

3.2. DSC analysis

The melting, boiling, and sublimation points of drug molecules either shift to different temperatures or disappear when these molecules are included in SB-β-CD cavities (Ascenso et al., 2011; de Azevedo Mde et al., 2011). The thermograms of HNK, SB-β-CD, HNK/CD PM, and HNK/CD COMP are shown in Fig. 3. HNK generated a sharp endothermic peak at 92 °C, indicating its melting point. The diagram of SB-β-CD exhibited an endothermic peak at 218 °C, due to the sample decomposition. In the case of HNK/CD PM, the melting peak of HNK at 92 °C and the endothermic peak of SB-β-CD were observed, indicating that there was no inclusion complex formed between HNK and SB-β-CD. However, no sharp peak was found in the thermogram of HNK/CD COMP at 92 °C, indicating the amorphous characteristic of HNK. The absence of the melting peak of HNK in the thermogram of HNK/CD COMP may have occurred because HNK was included in the SB-β-CD cavity.

3.3. FT-IR analysis

HNK/CD COMP was further analyzed by FT-IR spectroscopy. The spectra of HNK, SB-β-CD, HNK/CD PM, and HNK/CD COMP from 4000 to 400 cm^{-1} are shown in Fig. 4. The HNK spectrum showed the bands in the 3100 to 3000 cm^{-1} wave number regions, indicating the presence of —CH and —OH groups. A band was found at 1638 cm^{-1}, which can be assigned to alkene C=C present in HNK. The intense bands at 1498 and 1430 cm^{-1} were assigned to the stretching vibrations from the aromatic ring of honokiol molecule. Moreover, other bands were located at 1217 and 908 cm^{-1} (C—O) as well as at 989 and 825 cm^{-1} (C—C). The spectrum of SB-β-CD was mainly characterized by the intense bands at 3800 cm^{-1} to 3100 cm^{-1} caused by O—H stretching vibration. The band at 1643 cm^{-1} was ascribed to the δ-HOH bending of water molecules attached to SB-β-CD. The vibrations of —CH and —CH_2 groups appeared in the 3000 to 2800 cm^{-1} region. The sulfoxide stretched at 1046 cm^{-1} (Mahmoud, El-Feky, Kamel, & Awad, 2011; Venuti et al., 2013). In the case of HNK/CD PM, the spectrum was basically

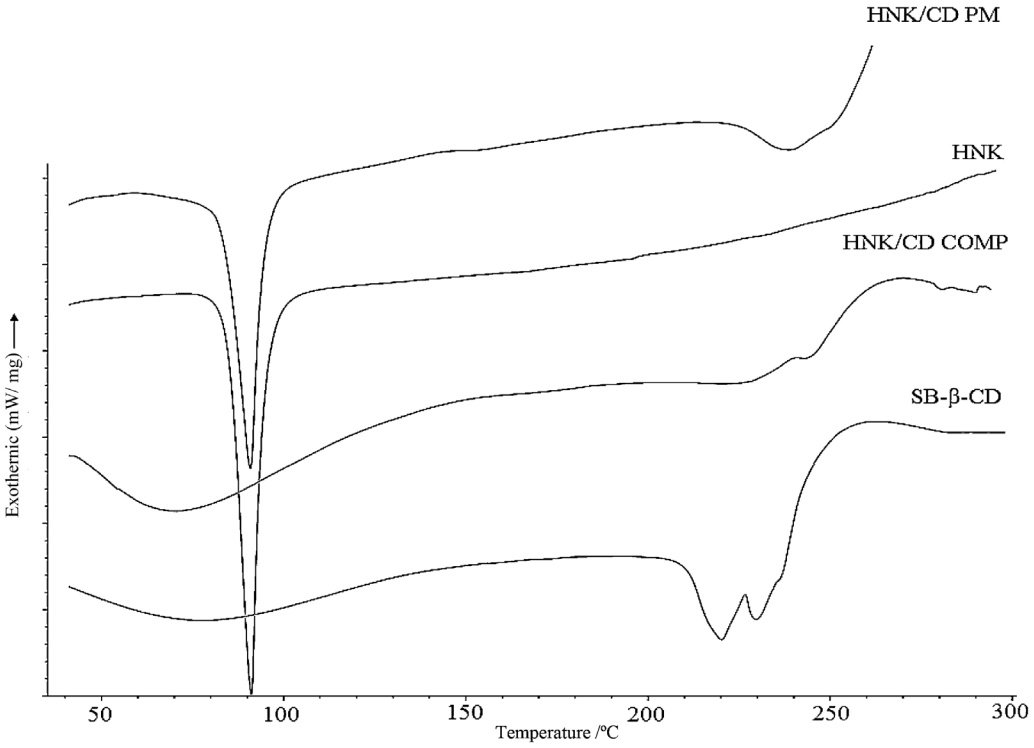

Fig. 3. Differential scanning calorimetry (DSC): (A) HNK; (B) HNK/CD PM; (C) SB-β-CD; (D) HNK/CD COMP.

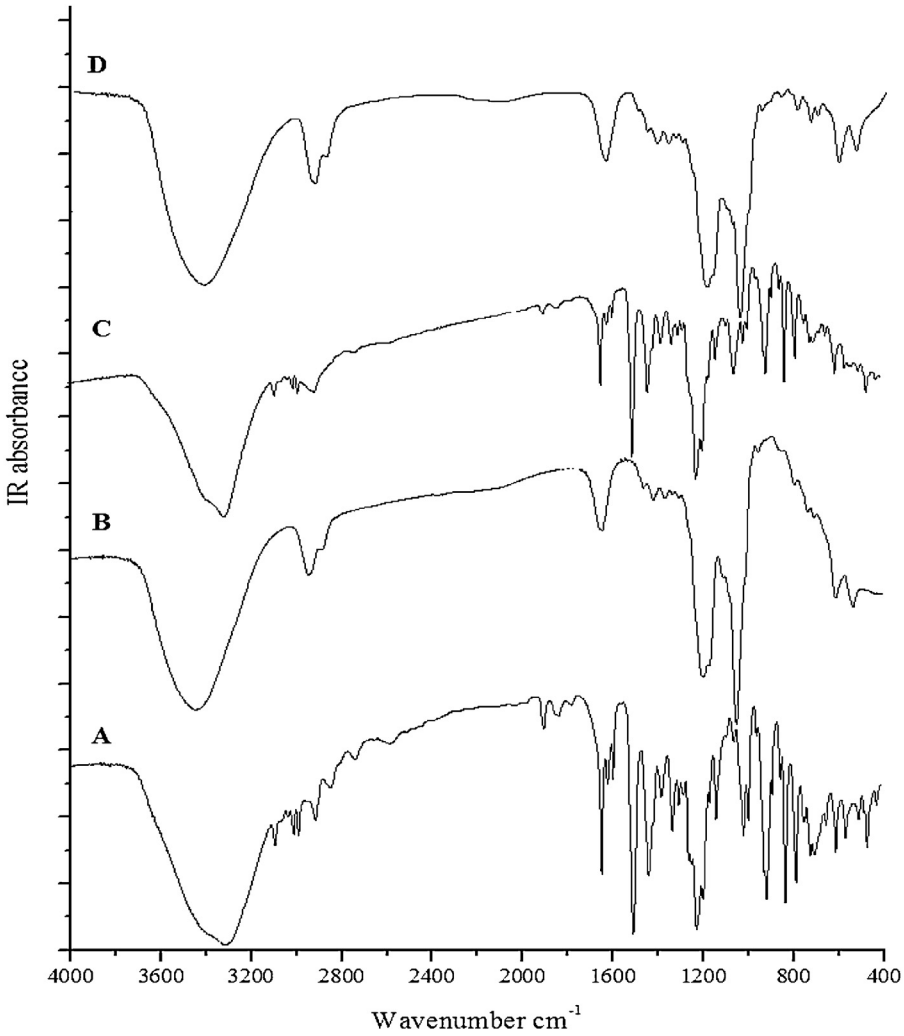

Fig. 4. FT-IR spectra of HNK (A), SB-β-CD (B), HNK/CD PM (C) and HNK/CD COMP (D).

composed of the overlapping peaks of HNK and SB-β-CD, and this spectrum showed a less intense absorption band at 1638 cm^{-1} than at other regions because of the low ratio of HNK in the physical mixture. This demonstrates that there was no interaction between drug and SB-β-CD. Compared with the HNK/CD PM, the spectrum of HNK/CD COMP showed relevant changes in intensities and widths of the typical absorption peaks, indicating the formation of a new compound between HNK and SB-β-CD (Venuti et al., 2014). A less intense absorption band was also observed at 1638 cm^{-1} in the spectrum of HNK/CD COMP, indicating that no interaction occurred between the C=C of HNK molecule and that of SB-β-CD molecule. Thus, C=C was not included in the cavity of SB-β-CD molecule. Therefore, only a part of the HNK molecule was possibly included in the cavity and the C=C portion of HNK molecule was not included.

3.4. In vitro release study

Fig. 5 shows the release curves of the free HNK, HNK/CD PM, and HNK/CD COMP in the 0.1 mM PBS (pH 7.4) containing SDS (0.5%). HNK/CD COMP exhibited a significantly higher release rate than that for the free HNK and HNK/CD PM. The cumulative release percentage of HNK/CD COMP at 0.5 h was >29% but <11% of the free HNK and 15% of HNK/CD PM. Furthermore, the cumulative release percentages of HNK/CD COMP and free HNK at 4 h were 82% and 28%, respectively.f_2 between the two curves of HNK/CD COMP and free HNK was 19.0 (<50) and that of HNK/CD PM and free HNK was 54.1(>50). These values indicated that the cumulative release profile of HNK/CD COMP was significantly different from that of the free HNK. However, no significant difference was found in HNK/CD PM and free HNK.

Different models, including Weibull, Higuchi (square root of time equation), Ritger-Peppas, Hixcon–Crowell model (cubic root law), zero-order, and first-order models, were utilized to fit the results of the mean release profiles. The model that fitted the release data more efficiently was selected on the basis of r, that is, a higher r corresponds to a better fit. For HNK/CD COMP, r of Weibull model ($\ln[1/1-Q] = 0.6872 \ln t + 0.7100$, $r = 0.9\ 914$)

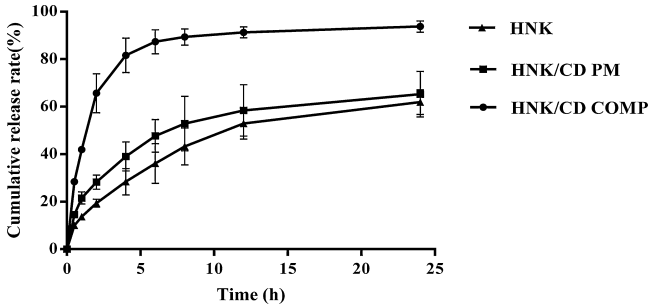

Fig. 5. Mean ($n = 3$) release curves of HNK/CD COMP (cycle), HNK/CD PM (square) and HNK (triangle) in 0.1 mM PBS (pH 7.4).

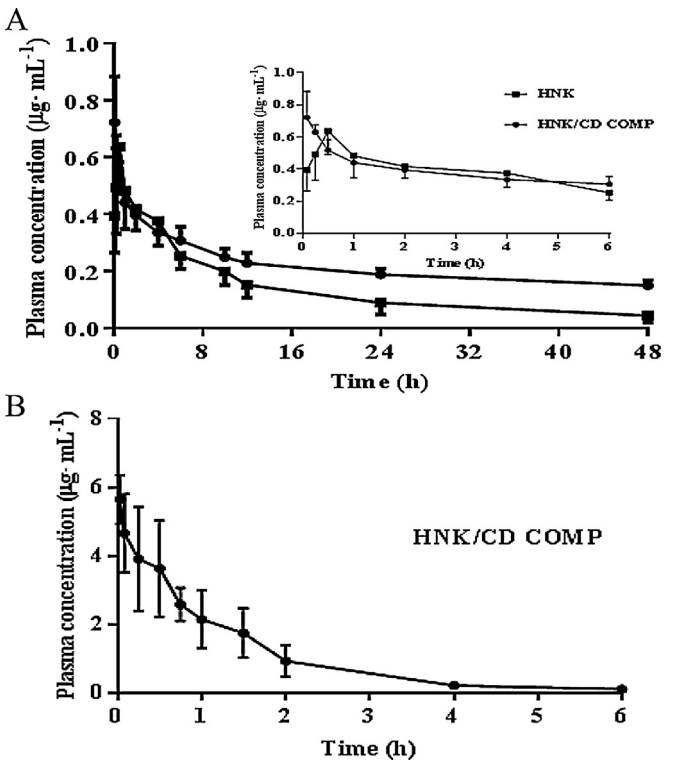

Fig. 6. Mean plasma concentration–time profiles of HNK in rats ($n = 6$): (A) HNK suspension and HNK/CD COMP solution after oral administration, (B) HNK/CD COMP solution via intravenous.

was the highest, indicating that the release profile of HNK/CD COMP best fitted the Weibull model among all of the models. The release profile of HNK/CD PM and HNK fitted well to the Ritger–Peppas model ($\ln Q = 0.4023 \ln t - 1.5494$, $r = 0.9\,870$ and $\ln Q = 0.5012 \ln t - 1.9532$, $r = 0.9\,953$, respectively).

3.5. Pharmacokinetic analysis of HNK in rats

HNK/CD COMP and HNK suspensions were administered to the male Sprague-Dawley rats to evaluate the enhanced bioavailability in vivo at post-oral administration. The validated HPLC method was employed in the pharmacokinetic analysis. A good linear relationship was obtained for HNK with concentration ranging from 0.0355 to 9.0909 $\mu g\,mL^{-1}$. The relative standard deviation of HNK for inter-day and intra-day precision and accuracy at low, medium and high concentration (0.0450, 2.2727 and 9.0909 $\mu g\,mL^{-1}$) was below 8.02%. The recoveries of HNK at the up three concentrations were 112.91, 106.84%, 100.88%. The limit of quantification (LOQ) for HNK was 0.0355 $\mu g\,mL^{-1}$. Satisfactory results were obtained after a single oral or intravenous dose were administered.

Fig. 6A shows the mean plasma concentration versus the time profiles of HNK after HNK/CD COMP and HNK suspensions were orally administered. Non-compartmental pharmacokinetic analysis was performed to evaluate HNK/CD COMP and HNK suspensions after these drugs were orally administered. The valuable pharmacokinetic parameters are listed in Table 2. The HNK/CD COMP group exhibited a higher HNK maximum plasma concentration (C_{max}) than that of the HNK suspension group (Fig. 6A; Table 2). AUC_{0-t} and C_{max} of the HNK/CD COMP group were 1.58 and 1.23 times higher than those of the HNK suspension group, respectively. This result indicated that SB-β-CD significantly enhanced the relative bioavailability of HNK ($p < 0.01$). The apparent volume of distribution (V) of HNK/CD COMP and HNK suspensions were 267.57 ± 97.48 and 191.93 ± 67.29, respectively

Table 2
The key non-compartmental parmacokinetic parameters of HK and HNK-SBECD ($n = 6$, $\bar{x} \pm s$).

Parameter	HNK (0.5%CMC-Na)	HNK-SBECD
AUC_{0-t} (mg h L^{-1})	6.59 ± 1.43	10.44 ± 0.75
$AUC_{0-\infty}$ (mg h L^{-1})	7.38 ± 1.74	15.27 ± 3.14
MRT_{0-t} (h)	12.83 ± 5.55	18.17 ± 1.15
$MRT_{0-\infty}$ (h)	17.66 ± 9.00	41.02 ± 14.38
C_{max} (mg L^{-1})	0.70 ± 0.21	0.86 ± 0.16
T_{max} (h)	0.47 ± 0.15	0.14 ± 0.08
$t_{1/2}$ (h)	13.00 ± 6.58	23.37 ± 5.69
V_d (L kg^{-1})	191.93 ± 67.29	267.57 ± 97.48
CL (L (h kg)$^{-1}$)	11.54 ± 3.56	4.14 ± 2.21

(Table 2). The body CL of HNK suspension was approximately three fold higher than that of HNK/CD COMP. T_{max} and $t_{1/2}$ of the HNK/CD COMP group displayed a statistically significant difference compared with those of the HNK suspension ($p < 0.05$). These results indicated that SB-β-CD significantly increased the absorption but delayed the elimination of HNK.

As a traditional administration route in clinical therapy, intravenous injection could work rapidly and prevent the first-pass effect. HNK could not be prepared into the solution injection because of its limited solubility. Using SB-β-CD, we found that the apparent solubility of HNK was increased significantly. Therefore, the preparation of HNK solution injection is possible. Hence, the pharmacokinetics of HNK/CD COMP after intravenous injection in rats was also investigated. The plasma concentration–time curve of HNK/CD COMP after administration to rats is shown in Fig. 6B, and their key pharmacokinetic parameters are listed as follows: $C_{max} = 5.31 \pm 0.84\,mg\,L^{-1}$, $T_{max} = 0.05 \pm 0.02$ h, and $AUC_{0-t} = 5.61 \pm 1.08$ mg h L^{-1}. These data are valuable references for the clinical application of HNK.

4. Conclusion

In this study, the inclusion complex of HNK and SB-β-CD was successfully prepared using a freeze–drying method. The solubility enhancement of HNK was investigated by the phase-solubility method, and the phase-solubility curves showed a typical A_L-type, indicating the formation of 1:1 (HNK:SB-β-CD) inclusion complex. Moreover, the formation of the inclusion complex was characterized by FT-IR and DSC. The apparent water solubility of HNK was significantly improved after this molecule formed a complex with SB-β-CD. The HNK/CD COPM exhibited a higher drug release rate than that of the free HNK in vitro. A comparative study of the pharmacokinetics between HNK/CD COPM and free HNK was also performed in rats. The in vivo results indicated that AUC_{0-t} and C_{max} of HNK/CD COPM resulted in an approximately 158% and 123% increase compared with those of the free HNK, respectively. These results suggest that SB-β-CD will be potentially useful in the delivery of poorly soluble drugs, such as HNK.

Acknowledgments

This project was supported by Natural Science Foundation Project of CQ CSTC (No. cstc2012jjA10021), the National Research Foundation for the Doctoral Program of Higher Education of China (No. 20125503120003), Scientific and Technological Research Program of Chongqing Municipal Education Commission (Grant nos. KJ110323 and KJ120307), Chongqing Board of Health Project (2013-2-060), Chongqing Yuzhong District Science and Technology Project (No. 20100203), Students' Research and Innovation Experimental Project of Chongqing Medical University (201244, 201229, 201217) and Students' Scientific Research Fund of "star of HIFU" (XS201309).

References

Al-Rawashdeh, N. A., Al-Sadeh, K. S., & Al-Bitar, M. B. (2010). Physicochemical study on microencapsulation of hydroxypropyl-beta-cyclodextrin in dermal preparations. *Drug Development and Industrial Pharmacy*, *36*(6), 688–697.

Albers, E., & Muller, B. W. (1995). Cyclodextrin derivatives in pharmaceutics. *Critical Reviews in Therapeutic Drug Carrier Systems*, *12*(4), 311–337.

Ascenso, A., Guedes, R., Bernardino, R., Diogo, H., Carvalho, F. A., Santos, N. C., et al. (2011). Complexation and full characterization of the tretinoin and dimethyl-beta-cyclodextrin complex. *AAPS PharmSciTech*, *12*(2), 553–563.

Brewster, M. E., & Loftsson, T. (2007). Cyclodextrins as pharmaceutical solubilizers. *Advanced Drug Delivery Reviews*, *59*(7), 645–666.

Carrier, R. L., Miller, L. A., & Ahmed, I. (2007). The utility of cyclodextrins for enhancing oral bioavailability. *Journal of Controlled Release*, *123*(2), 78–99.

Cheng, Z. (2012). Comparative studies on the interactions of honokiol and magnolol with human serum albumin. *Journal of Pharmaceutical and Biomedical Analysis*, *66*, 240–251.

Choi, J. H., Ha, J., Park, J. H., Lee, J. Y., Lee, Y. S., Park, H. J., et al. (2002). Costunolide triggers apoptosis in human leukemia U937 cells by depleting intracellular thiols. *Japanese Journal of Cancer Research*, *93*(12), 1327–1333.

Costa, P., & Sousa Lobo, J. M. (2001). Modeling and comparison of dissolution profiles. *European Journal of Pharmaceutical Sciences*, *13*(2), 123–133.

Danel, C., Azaroual, N., Chavaria, C., Odou, P., Martel, B., & Vaccher, C. (2013). Comparative study of the complex forming ability and enantioselectivity of cyclodextrin polymers by CE and 1H NMR. *Carbohydrate Polymers*, *92*(2), 2282–2292.

de Azevedo Mde, B., Tasic, L., Fattori, J., Rodrigues, F. H., Cantos, F. C., Ribeiro, L. P., et al. (2011). New formulation of an old drug in hypertension treatment: The sustained release of captopril from cyclodextrin nanoparticles. *International Journal of Nanomedicine*, *6*, 1005–1016.

FDA. (1997). *Guidance for industry: Dissolution testing of immediate-release solid oral dosage forms*. Food and Drug Administration, Center for Drug Evaluation and Research (CDER).

Garcia-Fernandez, M. J., Tabary, N., Martel, B., Cazaux, F., Oliva, A., Taboada, P., et al. (2013). Poly-(cyclo)dextrins as ethoxzolamide carriers in ophthalmic solutions and in contact lenses. *Carbohydrate Polymers*, *98*(2), 1343–1352.

Higuchi, T., & Connors, A. K. (1965). Phase solubility techniques. *Advances in Analytical Chemistry and Instrumentation*, *4*, 117–212.

Hu, L., Zhang, H., Song, W., Gu, D., & Hu, Q. (2012). Investigation of inclusion complex of cilnidipine with hydroxypropyl-beta-cyclodextrin. *Carbohydrate Polymers*, *90*(4), 1719–1724.

Irie, T., & Uekama, K. (1997). Pharmaceutical applications of cyclodextrins. III. Toxicological issues and safety evaluation. *Journal of Pharmaceutical Sciences*, *86*(2), 147–162.

Jadhav, P., Petkar, B., Pore, Y., Kulkarni, A., & Burade, K. (2013). Physicochemical and molecular modeling studies of cefixime–L-arginine–cyclodextrin ternary inclusion compounds. *Carbohydrate Polymers*, *98*(2), 1317–1325.

Kang, J. S., Lee, K. H., Han, M. H., Lee, H., Ahn, J. M., Han, S. B., et al. (2008). Antiinflammatory activity of methanol extract isolated from stem bark of *Magnolia kobus*. *Phytotherapy Research*, *22*(7), 883–888.

Lee, Y. J., Lee, Y. M., Lee, C. K., Jung, J. K., Han, S. B., & Hong, J. T. (2011). Therapeutic applications of compounds in the Magnolia family. *Pharmacology & Therapeutics*, *130*(2), 157–176.

Luke, D. R., Tomaszewski, K., Damle, B., & Schlamm, H. T. (2010). Review of the basic and clinical pharmacology of sulfobutylether-beta-cyclodextrin (SBECD). *Journal of Pharmaceutical Sciences*, *99*(8), 3291–3301.

Mahmoud, A. A., El-Feky, G. S., Kamel, R., & Awad, G. E. (2011). Chitosan/sulfobutylether-beta-cyclodextrin nanoparticles as a potential approach for ocular drug delivery. *International Journal of Pharmaceutics*, *413*(1–2), 229–236.

Pahuja, P., Kashyap, H., & Pawar, P. (2014). Design and evaluation of HP-beta-CD based voriconazole formulations for ocular drug delivery. *Current Drug Delivery*, *11*(2), 223–232.

Pralhad, T., & Rajendrakumar, K. (2004). Study of freeze-dried quercetin–cyclodextrin binary systems by DSC, FT-IR, X-ray diffraction and SEM analysis. *Journal of Pharmaceutical and Biomedical Analysis*, *34*(2), 333–339.

Rajendiran, N., & Siva, S. (2014). Inclusion complex of sulfadimethoxine with cyclodextrins: Preparation and characterization. *Carbohydrate Polymers*, *101*, 828–836.

Ruz, V., Froeyen, M., Busson, R., Gonzalez, M. M., Baudemprez, L., & Van den Mooter, G. (2012). Characterization and molecular modeling of the inclusion complexes of 2-(2-nitrovinyl) furan (G-0) with cyclodextrines. *International Journal of Pharmaceutics*, *439*(1–2), 275–285.

Shah, V., Lesko, L., Fan, J., Fleischer, N., Handerson, J., Malinowski, H., et al. (1997). FDA guidance for industry: Dissolution testing of immediate release solid oral dosage forms. *Dissolution Technologies*, *4*, 15–22.

Shah, V. P., Tsong, Y., Sathe, P., & Liu, J. P. (1998). In vitro dissolution profile comparison—Statistics and analysis of the similarity factor, f_2. *Pharmaceutical Research*, *15*(6), 889–896.

Singh, R. M., Kumar, A., & Pathak, K. (2013). Thermally triggered mucoadhesive in situ gel of loratadine: Beta-cyclodextrin complex for nasal delivery. *AAPS PharmSciTech*, *14*(1), 412–424.

Stella, V. J., & He, Q. (2008). Cyclodextrins. *Toxicologic Pathology*, *36*(1), 30–42.

Thompson, D. O. (1997). Cyclodextrins—Enabling excipients: Their present and future use in pharmaceuticals. *Critical Reviews in Therapeutic Drug Carrier Systems*, *14*(1), 1–104.

Tiwari, G., Tiwari, R., & Rai, A. K. (2010). Cyclodextrins in delivery systems: Applications. *Journal of Pharmacy and Bioallied Sciences*, *2*(2), 72–79.

Uekama, K. (2004). Design and evaluation of cyclodextrin-based drug formulation. *Chemical & Pharmaceutical Bulletin (Tokyo)*, *52*(8), 900–915.

Venuti, V., Cannava, C., Cristiano, M. C., Fresta, M., Majolino, D., Paolino, D., et al. (2013). A characterization study of resveratrol/sulfobutyl ether-beta-cyclodextrin inclusion complex and in vitro anticancer activity. *Colloids and Surfaces B: Biointerfaces*, *115C*, 22–28.

Venuti, V., Cannava, C., Cristiano, M. C., Fresta, M., Majolino, D., Paolino, D., et al. (2014). A characterization study of resveratrol/sulfobutyl ether-beta-cyclodextrin inclusion complex and in vitro anticancer activity. *Colloids and Surfaces B: Biointerfaces*, *115*, 22–28.

Wang, X., Luo, Z., & Xiao, Z. (2014). Preparation, characterization, and thermal stability of beta-cyclodextrin/soybean lecithin inclusion complex. *Carbohydrate Polymers*, *101*, 1027–1032.

Weeks, B. S. (2009). Formulations of dietary supplements and herbal extracts for relaxation and anxiolytic action: Relarian. *Medical Science Monitor*, *15*(11), RA256–RA262.

Yamaguchi, N., Satoh-Yamaguchi, K., & Ono, M. (2009). In vitro evaluation of antibacterial, anticollagenase, and antioxidant activities of hop components (*Humulus lupulus*) addressing acne vulgaris. *Phytomedicine*, *16*(4), 369–376.

Zhang, J., & Ma, P. X. (2013). Cyclodextrin-based supramolecular systems for drug delivery: Recent progress and future perspective. *Advanced Drug Delivery Reviews*, *65*(9), 1215–1233.

Zhang, W., Gong, X., Cai, Y., Zhang, C., Yu, X., Fan, J., et al. (2013). Investigation of water-soluble inclusion complex of hypericin with beta-cyclodextrin polymer. *Carbohydrate Polymers*, *95*(1), 366–370.